Signals from Clustered Ion Channels

P. Jung, S. Zeng, and J.W. Shuai

Department of Physics and Astronomy and Institute for Quantitative Biology
Ohio University, Athens OH 45701, USA

Abstract. Clustering of ion channels is a common phenomenon, yet it is not well understood. While several explanations for channel clustering have been suggested, we propose a new theory that is based on information theoretic reasoning and is thus generic and may apply very generally.

1 Introduction

Clustering of ion channels is a very common phenomenon in nature. It occurs naturally in myelinated neurons, where the active sodium channels are concentrated at the *nodes of Ranvier* acting as a signal booster. But it also in neurons that are *not myelinated*, e.g. in some neuron types in the retina [1]. In these types of neurons, there is no obvious geometric reason for the clustering. As another example, the release of Ca^{2+} from the endoplasmic (or sarcoplasmic) reticulum, is controlled by *small* clusters of Ca^{2+}-release channels, that often contain no more than 20–50 channels. While it is not understood why the ion channels are clustered, a number of theories and theoretical models have been put forward. Some of them involve attractive interactions between the channel proteins [2], the organization of the membrane in micro-domains ("rafts") with different structures where some structures are more likely to host channel proteins than others [3], or the involvement of the cytoskeleton by locally anchoring the channels by a sub-membrane undercoat [1]. A novel idea towards the solution of this puzzle is based on the capability of information transmission of groups of ion channels [4,5,6]. In these papers, it has been shown that small signals may be better detected by smaller clusters. The size of the ion channel clusters determines (for small clusters in a non-trivial way) the magnitude of the fluctuations and thus – via the effect of stochastic resonance – a small signal can be enhanced.

Intracellular calcium signaling is based on the release of calcium from intracellular stores by small clusters of release channels that may not include more than 20–50 channels. We propose that the small size of the cluster enhances the calcium release stimulated *by small numbers of agonist* binding to the receptors. A simple stochastic theory predicts optimal cluster sizes that are compatible with experimental results.

B. Kramer (Ed.): Adv. in Solid State Phys. **43**, pp. 605–616, 2003.
© Springer-Verlag Berlin Heidelberg 2003

2 Optimal Cluster Sizes in Neuronal Ion Channels Clusters

Since there is a great variety in the distribution and kinds of ion channels relevant for transmission of electrical signals in the nervous system, we are selecting as model channels those, that have been identified in the squid axon (although they are not clustered there). Most important are the sodium and potassium channels. Each potassium channel has four identical subunits (gates) that are either closed or open. The opening and closing rates $\alpha_{\rm K}(v)$ and $\beta_{\rm K}(v)$, respectively, for each subunit are given by [7]

$$\alpha_{\rm K}(v) = \frac{0.01(10-v)}{\exp\left((10-v)/10\right)-1} \quad , \quad \beta_{\rm K}(v) = 0.125\exp\left(-\frac{v}{80}\right), \tag{1}$$

where v refers to the cross-membrane potential. The opening and closing processes of the subunits are assumed to be Markovian and described by the two-state master equation for the open-probability of a subunit

$$\dot{p}_n(t) = -\left(\alpha_{\rm K}(v)+\beta_{\rm K}(v)\right)p_n(t) + \alpha_{\rm K}(v)\,. \tag{2}$$

The entire channel is open when all four subunits are open.

The sodium channel is composed of three identical (fast) subunits that – similar to the potassium channel subunits – tend to open when the cross-membrane voltage is increasing, i.e.

$$\alpha^f_{\rm Na}(v) = \frac{0.1(25-v)}{\exp\left((25-v)/10\right)-1} \quad , \quad \beta^f_{\rm Na}(v) = 4.0\exp\left(-\frac{v}{18}\right) \tag{3}$$

with the corresponding two state master equations for the state of the gates

$$\dot{q}_n(t) = -\left(\alpha^f_{\rm Na}(v)+\beta^f_{\rm Na}(v)\right)q_n(t) + \alpha^f_{\rm Na}(v)\,. \tag{4}$$

But it also comprises a (slow) deactivation gate that tends to close with increasing trans-membrane voltage. The opening and closing rates of the deactivation gates are given by

$$\alpha^s_{\rm Na}(v) = 0.07\exp\left(-\frac{v}{20}\right) \quad , \quad \beta^s_{\rm Na}(v) = \frac{1}{\exp\left((30-v)/10\right)+1}\,, \tag{5}$$

with the associated two-state master equation describing the state of the in-activation gate

$$\dot{q}_4(t) = -\left(\alpha^s_{\rm Na}(v)+\beta^s_{\rm Na}(v)\right)q_4(t) + \alpha^s_{\rm Na}(v)\,. \tag{6}$$

A sodium channel is open when all three fast gates are open and the inactivation gate is open. In all equations above, the trans-membrane potential is measured in millivolts (mV), and the time is measured in milliseconds (ms).

A cluster of ion channels is made up of a number N_K of potassium channels and $N_{\rm Na}$ of sodium channels that are close enough that they all share

the same (not fixed) trans-membrane potential. To obtain a rough estimate of the allowed distances we employ linear cable theory. Assuming that the cluster under consideration is located on an axon and that the axon (a long thin object) can be treated as a one-dimensional cable, the cable equation for the transmembrane voltage $v(x,t)$ along the cable (x-direction) reads

$$\tau \frac{\partial v(x,t)}{\partial t} = -I_{\text{ion}} R_m + \lambda_m^2 \frac{\partial^2 v(x,t)}{\partial x^2}\,, \tag{7}$$

where for the giant squid axon (our model system), $\lambda_m = 0.65\,\text{cm}$, $R_m = 10^3 \Omega\,\text{cm}^2$ and $\tau = 1\,\text{ms}$. The term I_{Ion} contains all specific ionic transmembrane currents and a leakage current that lumps all other ionic currents.

The linear extent of a ion-channel cluster with a shared trans-membrane potential therefore should be smaller than the typical length scale of the system $\lambda_m = 0.65cm$. Since a two-dimensional "cable equation" would factorize into two cable equations, a cluster size should be much less than $0.4\,\text{mm}^2$ in order that the approximation of uniform voltage to apply. In this paper we only consider cluster sizes of up to several hundred μm^2 and we thus stay well within the regime where a shared transmembrane potential is a very good approximation. Thus, within one ion channel cluster, the diffusion term on the right hand side of the cable equation vanishes and we wind up with an ordinary differential equation for the transmembrane potential which we re-write as

$$C\frac{dv}{dt} = -g_{\text{K}}(v - v_{\text{K}}) - g_{\text{Na}}(v - v_{\text{Na}}) - g_l(v - v_l) + I_{\text{ext}}\,, \tag{8}$$

with the conductance of the sodium system, potassium system and leakage system given by $g_{\text{K}}, g_{\text{Na}}, g_l$, respectively. C denotes the membrane capacitance and $v_{\text{K}}, v_{\text{Na}}$ and v_{L} the Nernst potentials of the ionic systems. Assuming that the densities of the potassium channels ρ_{K} and sodium channels ρ_{Na} are homogeneous throughout the cluster of area A, we can express g_{K} and g_{Na} in terms of the conductance of single open channels $\gamma_{\text{K}}, \gamma_{\text{Na}}$, i.e.

$$\begin{aligned}
\frac{g_{\text{K}}}{A} &= \frac{N_{\text{K}}^{\text{open}}\gamma_{\text{K}}}{A} = \frac{N_{\text{K}}^{\text{open}}}{N_{\text{K}}}\rho_{\text{K}}\gamma_{\text{K}} \\
\frac{g_{\text{Na}}}{A} &= \frac{N_{\text{Na}}^{\text{open}}\gamma_{\text{Na}}}{A} = \frac{N_{\text{Na}}^{\text{open}}}{N_{\text{Na}}}\rho_{\text{Na}}\gamma_{\text{Na}}\,.
\end{aligned} \tag{9}$$

Dividing (8) by the cluster area, one finds

$$\begin{aligned}
C\frac{dv}{dt} = &-\frac{N_{\text{K}}^{\text{open}}}{N_{\text{K}}}\rho_{\text{K}}\gamma_{\text{K}}(v - v_{\text{K}}) \\
&-\frac{N_{\text{Na}}^{\text{open}}}{N_{\text{Na}}}\rho_{\text{Na}}\gamma_{\text{Na}}(v - v_{\text{Na}}) - g_l(v - v_l) + I_{\text{ext}}\,.
\end{aligned} \tag{10}$$

The fraction of open channels can be obtained at each time step by using a Monte-Carlo type technique put forward in [8].

As a result of this Monte-Carlo type procedure, the number of open channels (potassium and sodium) is determined and can be inserted into Eq.(10) which is then integrated by one time step of $10\mu s$ by using a first order solver. For the channel densities we use $\rho_{\mathrm{Na}} = 60/\mu m^2$ and $\rho_{\mathrm{K}} = 20/\mu m^2$.

Subsequent updating of the channel-states and integration of Eq.(10) leads to the membrane voltage as a function of time. A typical trajectory is shown in Fig. 1.

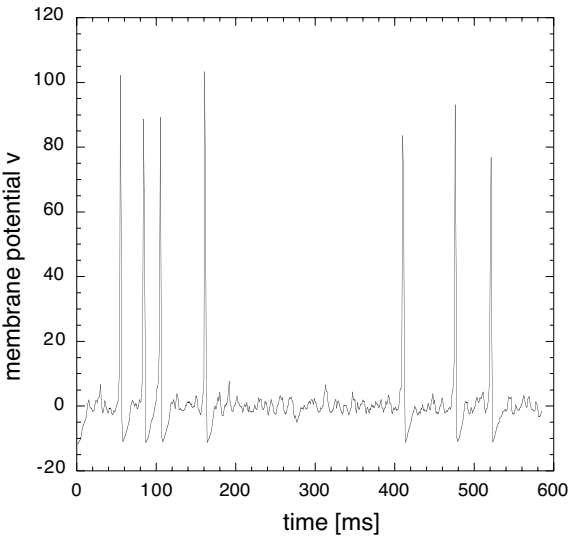

Fig. 1. A spike train generated spontaneously by 1000 potassium and 3000 sodium channels in one cluster is shown. The fluctuations of the membrane potential during quiescent intervals is about 10 mV, i.e. more than 10% of the actual resting potential of about -70 mV

2.1 Spontaneous Firing Rates

In Fig. 2, the average time-interval between two successive action potentials is shown as a function of the cluster size. For small cluster sizes, the firing rate *increases* with increasing cluster size. Only after the cluster size exceeds about $1\mu m^2$, an increasing cluster size results in a decreasing spontaneous firing rate.

2.2 Variance and Firing Rates

In Fig. 3, we show the standard deviation from the average firing interval normalized by the average firing interval as a function of the cluster size. This measure is called the *Fano-factor* and is used sometimes to describe

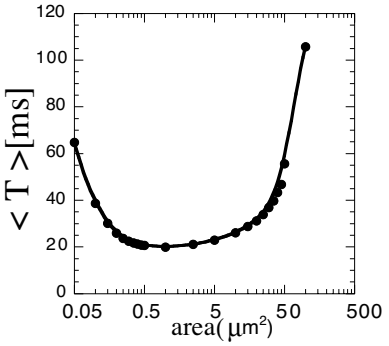

Fig. 2. The average interval between two consecutive spontaneous spikes is shown as a function of the cluster size N

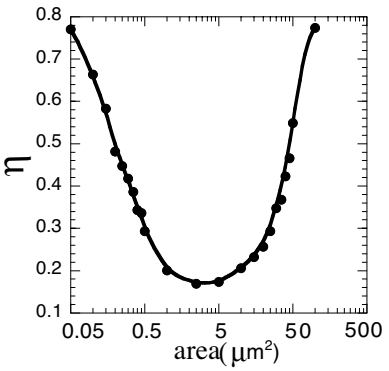

Fig. 3. Form of the Fano factor $\eta = \left\langle (T - \langle T \rangle)^2 \right\rangle / \langle T \rangle^2$ as a function of the cluster size N

the regularity of the spike train. This Fano factor η is shown in Fig. 3 as a function of the cluster size. For vanishing synaptic noise this measure exhibits a minimum roughly where the firing rate exhibits a maximum.

2.3 Response to Weak Signals

In the limit of large cluster sizes, the deterministic Hodgkin-Huxley equations require the amplitude of injected currents to exceed a threshold (which in general depends on the frequency content of the signal). Thus a signal that does not overcome this threshold *will not* be encoded in a spike train. Decreasing the cluster size will increase the fluctuations of the membrane potential (as it is evident from Fig. 2). When the membrane voltage fluctuations add favorably to the (sub-threshold) external signal an encoding takes place as random sampling of the subthreshold signal. When the fluctuations become too big, i.e. the area of the cluster too small, the fluctuations of the transmembrane potential over-dominate the signal and the neuronal spike train mostly encodes the noise and not the signal.

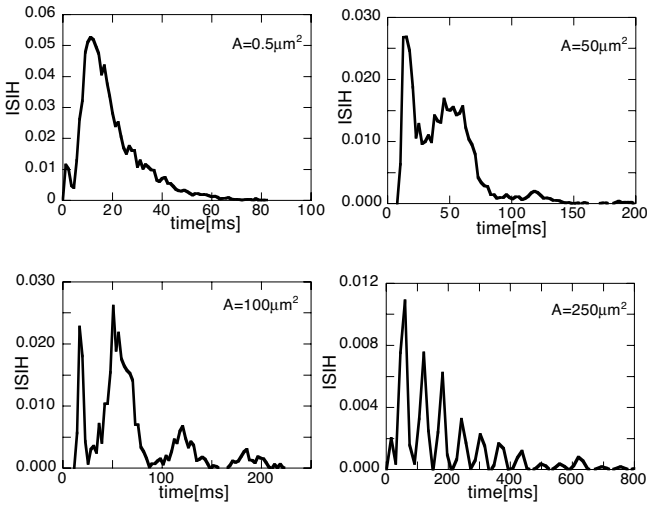

Fig. 4. The interspike interval histograms (ISIH) are shown for a subthreshold sinusoidal signal (11) for cluster areas of $0.5\mu m^2, 5\mu m^2, 100\mu m^2$ and $250\mu m^2$

This effect is demonstrated in Fig. 4, where we show the interspike-interval histograms (ISIH) of the neuronal spike train at various clustersizes when an external current of the form

$$I_{\text{ext}} = A\cos\left(\frac{2\pi t}{T}\right) \tag{11}$$

is applied, where $A = 2\mu$ A/cm^2 and $T = 60$ ms. A peak of the ISIH at the period of the external signal indicates encoding of the signal. Since the ISIH's in Fig. 4 are normalized, the height of the peak (if any) at $T = 60ms$ can be used as a measure of encoding. Best encoding takes place for the injected signal under consideration at a cluster area of about $100\mu m^2$.

Another remarkable finding is that the ISIH at small cluster sizes (see the left upper panel of Fig. 4) exhibits an additional peak at very small intervals, indicating that the concept of refractory period that is characteristic for the macroscopic deterministic systems seems to collapse.

3 Optimal Cluster Sizes for Intracellular Ca^{2+} Signaling

Many important cellular functions are regulated by intra- and intercellular Ca^{2+} signals. They are involved in the insulin production of pancreatic β–cells [9], in the enzyme secretion in liver cells (for a review, see e.g. [10]) and for the early response to injury of brain tissue [11] and corneal epithelia [12]. Recent new insights into the biophysical mechanism of intracellular

Ca^{2+} release have revealed that the actual release sites are discrete and as small as about 100 nm indicating that mesoscopic methods are necessary for realistic models of Ca^{2+}. Consequences of the discreteness of the release clusters for Ca^{2+} wave formation have been explored in [13] and [14]. In this paper, we show that the clustering of the release channels can resonantly enhance the sensitivity of the calcium signaling pathway by exploiting internal fluctuations.

Most of the Ca^{2+} that constitutes the signal is released from intracellular stores such as the endoplasmic reticulum (ER) into the intracellular space through the Inositol 1,4,5-Trisphosphate (IP_3) receptor. The IP_3 receptor (IP_3R) is modeled [15] by three identical subunits that each have three binding sites: one for the messenger molecule IP_3 (m gate), one activating site (n gate) for Ca^{2+} and one inactivating site (h gate) for Ca^{2+}. In order for a subunit to conduct Ca^{2+}, only the IP_3 and the activating Ca^{2+} binding site need to be occupied. The entire IP_3R is conducting if three subunits are conducting. The Ca^{2+} binding site invokes an autocatalytic mechanism of Ca^{2+} release (Ca^{2+} induced Ca^{2+} release) giving rise to a rapidly increasing intracellular Ca^{2+} concentration if the concentration of IP_3 exceeds a certain threshold. When the inactivation Ca^{2+} binding sites become occupied and the IP_3Rs close, the Ca^{2+} pumps remove Ca^{2+} from the intracellular space, which is necessary since elevated concentrations of Ca^{2+} are toxic for the cell. Once the Ca^{2+} concentration is low and IP_3 is present in sufficient concentration, calcium induced calcium release will rapidly increase intracellular calcium levels giving rise to oscillatory calcium signals. The oscillatory nature of the Ca^{2+} signals suggests that the primary information content of the Ca^{2+} signals is their frequency [16]. In previous work it has been reported that globally IP_3-mediated Ca^{2+} signals can be devolved into localized Ca^{2+} release events due to *clustered distributions* of IP_3Rs [17] with only a few tens of IP_3Rs per cluster and a size of about $100nm$, indicating that thermal open-close transitions of single IP_3R's are essential. Observations of signals of differing magnitudes first suggested a hierarchy of calcium signalling events, with smaller blips representing fundamental events involving opening of single IP_3R and the larger sparks or puffs being elementary events resulting from the opening of small groups of IP_3Rs [18,17]. Improved spatial and temporal resolution recordings, however, have revealed that there is not a clear distinction between fundamental and elementary events [17,19]. It is suggested that the localized calcium release varies in a continuous fashion due to *stochastic variation* in both numbers of channels recruited and durations of channel openings.

Our study is based on the Li-Rinzel Model [20], a two-variable simplification of the DeYoung-Keizer model [15] where the fast variables m, n have been replaced by their quasi equilibrium values m_∞ and n_∞. According to this model, the calcium flux from the ER to the intracellular space is driven

by the Ca^{2+} gradient, i.e.

$$\frac{d[Ca^{2+}]}{dt} = -I_{\mathrm{Ch}} - I_{\mathrm{P}} - I_{\mathrm{L}}, \tag{12}$$

$$\frac{dh}{dt} = \alpha_h(1-h) - \beta_h h\,, \tag{13}$$

with

$$I_{\mathrm{Ch}} = c_1 v_1 m_\infty^3 n_\infty^3 h^3([\mathrm{Ca}^{2+}] - [\mathrm{Ca}^{2+}]_{\mathrm{ER}}) \tag{14}$$

$$I_{\mathrm{P}} = \frac{v_3[\mathrm{Ca}^{2+}]^2}{k_3^2 + [\mathrm{Ca}^{2+}]^2} \tag{15}$$

$$I_{\mathrm{L}} = c_1 v_2([\mathrm{Ca}^{2+}] - [\mathrm{Ca}^{2+}]_{\mathrm{ER}})\,. \tag{16}$$

Here, $[\mathrm{Ca}^{2+}]$ denotes the intracellular Ca^{2+} concentration, $[\mathrm{Ca}^{2+}]_{\mathrm{ER}}$ the Ca^{2+} concentration in the ER, and h a slow inactivation variable. I_{Ch} denotes Ca^{2+} efflux from intracellular stores through IP_3R channels, I_{P} the ATP-dependent Ca^{2+} flux from the intracellular space back to the stores, and I_{L} represents the leak flux. The slow Ca^{2+} inactivation process depends on both the concentration of IP_3 and Ca^{2+} via the rate constants

$$\alpha_h = a_2 d_2([\mathrm{IP}_3] + \mathrm{d}_1)/([\mathrm{IP}_3] + \mathrm{d}_3)\ ,\ \beta_{\mathrm{h}} = \mathrm{a}_2[\mathrm{Ca}^{2+}]. \tag{17}$$

The other parameters are $m_\infty = [\mathrm{IP}_3]/([\mathrm{IP}_3] + \mathrm{d}_1)$, $n_\infty = [\mathrm{Ca}^{2+}]/([\mathrm{Ca}^{2+}] + \mathrm{d}_5)$, c_1=0.185, $v_1 = 6\mathrm{s}^{-1}$, $v_2 = 0.11\mathrm{s}^{-1}$, $v_3 = 0.9\mu\mathrm{Ms}^{-1}$, $k_3 = 0.1\mu\mathrm{M}$, $d_1 = 0.13\mu\mathrm{M}$, $d_2 = 1.049\mu\mathrm{M}$, $d_3 = 0.9434\mu\mathrm{M}$, $d_5 = 0.08234\mu\mathrm{M}$, and $a_2 = 0.2\mu\mathrm{M}^{-1}\mathrm{s}^{-1}$. The total amount of Ca^{2+} is conserved via the Ca^{2+} concentration in ER with $[\mathrm{Ca}^{2+}]_{\mathrm{ER}} = (\mathrm{c}_0 - [\mathrm{Ca}^{2+}])/\mathrm{c}_1$ with $c_0 = 2.0\mu\mathrm{M}$. The concentration of IP_3 denoted by $[\mathrm{IP}_3]$ is a control parameter.

The form of Eq. (13) suggests that the inactivation process for each IP_3R can be modeled as a stochastic process where $h = 1$ describes the open IP_3R and $h = 0$ describes the closed IP_3R (i.e. no calcium current through the IP_3R) – constituting the *stochastic Li-Rinzel model*. The power three of h in Eq. (12) indicates the three subunits of the IP_3R and thus three inactivation h gates. Each gate can be in two states, the open (unbound) and closed (bound) state. Since the h-gates are the slowest gates, we assume that switching between the two states can be approximated by a two-state Markov process with the opening rate of α_h and the closing rate β_h. The IP_3R is conducting if all three h-sites are unbound. The Ca^{2+} flux through the IP_3R in the kinetic model is then given by the modified form of Eq. (14)

$$I_{\mathrm{Ch}} = c_1 v_1 m_\infty^3 n_\infty^3 \frac{N^{h-\mathrm{Open}}}{N}\left([\mathrm{Ca}^{2+}] - [\mathrm{Ca}^{2+}]_{\mathrm{ER}}\right), \tag{18}$$

where N and $N^{h-\mathrm{Open}}$ indicate the total number of IP_3Rs and the number of h-open receptors in the cluster, respectively. Eqs. (12)–(17) represent the deterministic limit of the stochastic scheme Eqs.(12), (15)–(18) for a large

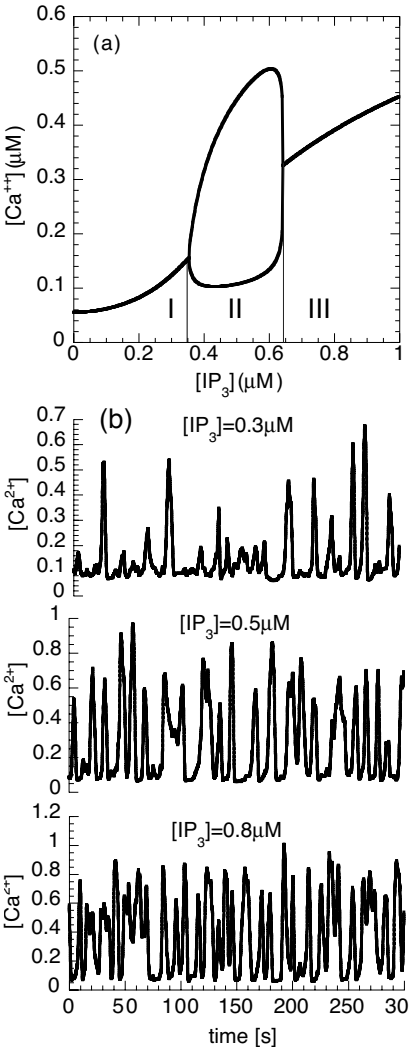

Fig. 5. The bifurcation diagram of the deterministic Li-Rinzel model (**a**) and calcium signals generated by a cluster of 20 IP_3Rs (**b**)

number N of channels. The release of Ca^{2+} in the stochastic Li-Rinzel model is a collective event of a number of globally coupled channels (via the common Ca^{2+} concentrations) with stochastic opening and closing dynamics. Each gate is simulated explicitly by two-state Markov processes with opening and closing rates α_h and β_h, respectively.

In the deterministic limit (i.e. $N \to \infty$), the two-variable Li-Rinzel model has one stable fixed point for $[IP_3] < 0.354\mu M$ and $[IP_3] > 0.642\mu M$. At $[IP_3]=0.354\ \mu M$ and $[IP_3]=0.642\mu M$ Hopf bifurcations occur so that $[Ca^{2+}]$ is oscillating for $0.354\mu M<[IP_3]<0.642\mu M$ (Fig. 5a). Under normal conditions

$[IP_3]$ is below the critical value 0.354μM and the deterministic model with a fixed point does not permit calcium signaling.

In Fig. 5b, traces of a Ca^{2+} signal released from a cluster with 20 IP_3Rs are shown for three values of $[IP_3]$ in the three deterministically distinguished regimes I,II,III (see Fig. 5a). The Ca^{2+} signals consists of stochastic sequences of Ca^{2+} release events (calcium puffs) in all three regimes (I,II,III) with a continuum of amplitudes and durations. The regimes I,II and III are not well distinguishable for these small clusters. Most importantly for the purpose of this paper, the Ca^{2+} puffs for $[IP_3] < 0.354\mu M$ constitute a Ca^{2+} signal with a frequency content. To determine the degree of periodicity of the Ca^{2+} released from a cluster, we compute the normalized power spectrum

$$S_s(\omega) = \frac{1}{T} \frac{\left| \int_0^T \left([Ca^{2+}](\tau) - \langle [Ca^{2+}] \rangle \right) \exp\left(-2\pi i \omega \tau\right) d\tau \right|}{\sqrt{\langle \left([Ca^{2+}] - \langle [Ca^{2+}] \rangle \right)^2 \rangle}}, \tag{19}$$

where the length of the observation interval T is 5000 s for all data presented in this paper. In Fig. 6, we show the normalized power spectra $S(\omega)$ at various sizes N of the release cluster. For very small clusters (e.g. $N = 2$ in Fig. 6a) and very large clusters (e.g. $N = 10,000$ in Fig. 6c)), the power spectrum does not exhibit a peak and thus the release of Ca^{2+} is dominated by stochastic

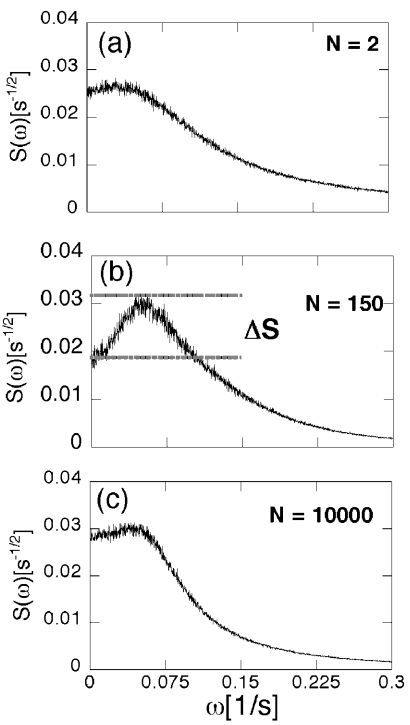

Fig. 6. Power spectra $S(\omega)$ of the Ca^{2+} signal released by clusters of (**a**) $N = 2$, (**b**) N=150, and (**c**) N=10,000 IP_3Rs at $[IP_3]$=0.30 μM

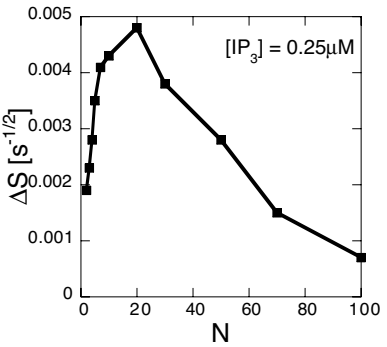

Fig. 7. The elevation of the power spectrum ΔS as a function of N at $[IP_3]$=0.25 μM

events. In between, however, a peak in the power spectrum (Fig. 6b) indicates periodicity in calcium release. The *strength* of the peak is characterized by the elevation of the peak ΔS which is shown in Fig. 7 as a function of the size of the cluster N for $[IP_3]$=0.25 μM. The elevation of the power spectrum goes through a maximum at $N \approx 20$. Typical recorded values of $[IP_3]$ range between $0.15\mu M - 0.25\mu M$. In this context it is interesting to note that the coherence for $[IP_3]$=0.25 μM peaks at $N = 20$ which is considered a realistic cluster size (see also [21]). To summarize, the overall coherence of the Ca^{2+} signal exhibits a maximum at a cluster size that depends on the concentration of IP_3. For IP_3 concentrations closer to the Hopf-bifurcation ($[IP_3]$=0.354μM), the maximum coherence is achieved for larger clusters of IP_3Rs and vice versa.

Acknowledgements

This material is based upon work supported by the National Science Foundation under Grant No. IBN-0078055.

References

1. C. Hildebrand and S.Waxman, Brain Research, **258** 23(1983). 605
2. C. Guo and H. Levine, Biophysical Journal **77**, 2358 (1999). 605
3. H. Grassme, V. Jendrossek, J. Bock, A. Riehle, E. Gulbins, Journal of Immunology, **168**, 298 (2002); J.R. Cochran, D. Aivazian, T.O. Cameron, L.J. Stern, Trends in Biochemical Sciences, **26**, 304 (2001); G. Vereb, J. Matko, G. Vamosi, S.M. Ibrahim, E. Magyar, S. Varga, J. Szollosi, A. Jenei, R. Gaspar, T.A. Waldmann, S. Damjanovich, PNAS, **97**, 6013 (2000); S. Damjanovich, L. Bene, J. Matko, L. Matyus, Z. Krasznai, G. Szabo, C. Pieri, R. Gaspar R, J. Szollosi, Biophysical Chemistry **82**, 99 (1999). 605
4. P. Jung and J. W. Shuai, Europhys. Lett. **56**, 29 (2001). 605
5. G. Schmid, I. Goychuk and P. Hänggi, Europhys. Lett. **56**, 22 (2001). 605
6. J.W. Shuai and P. Jung, Phys. Rev. Lett., **88**, 681021 (2002). 605
7. A.L. Hodgkin and A.F. Huxley, J. Physiol.(London), **117**, 500 (1952). 606

8. E. Schneidman, B. Freedman, I. Segev, Neural Computation, **10**, 1679 (1998). 607
9. T. R. Chay and J. Keizer, Biophys. J. **42**, 181 (1983). 610
10. G. Dupont, S. Swillens, C. Clair, T. Tordjmann, and L. Combettes, Biochimica et Biophysica Acta, **1498**, 134 (2000). 610
11. A. H. Cornell-Bell, S. M. Finkbeiner, M. S. Cooper, and S.J. Smith, Science **247**, 470 (1990). 610
12. V.E. Klepeis, A.H. Cornell-Bell, and Vickery Trinkaus-Randall, J. Cell Sci., **114**, 4185 (2001). 610
13. M. Falcke, L. Tsimring and H. Levine, Phys. Rev. **E62**, 2636 (2000). 611
14. J. Keizer and G.D. Smith, Biophysical Chemistry, **72**, 87 (1998). 611
15. G. W. D. Young and J. Keizer. Proc. Natl. Acad. Sci. USA. **89**, 9895 (1992). 611
16. P. D. Koninck and H. Schulman, Science, **279**, 227 (1998); R. E. Dolmetsch, K. Xu, and R. S. Lewis, Nature, **392**, 933 (1998). 611
17. M. Bootman, E. Niggli, M. Berridge, and P. Lipp, The Journal of Physiology, **499**, 307 (1997). 611
18. P. Lipp, and E. Niggli, Journal of Physiology **508**, 801 (1996); H. Cheng, W. J. Lederer, and M. B. Cannell, Science, **262**, 740 (1993). 611
19. X. Sun, N. Callamaras, J. S. Marchant, and I Parker, *Journal of Physiology*, **509**, 67 (1998); D. Thomas, P. Lipp, M. J. Berridge, and M. D. Bootman, J. Biol. Chem. **273**, 27130 (1998); J. S. Marchant and I. Parker, The EMBO Journal, **20**, 65 (2001); L. L. Haak, L. Song, T. F. Molinski, I. N. Pessah, H. Cheng, and J. T. Russell, Journal of Neuroscience, **21**, 3860 (2001). 611
20. Y. Li and J. Rinzel, J. Theor. Biol. **166**, 461 (1994). 611
21. S. Swillens, G. Dupont, L. Combettes, and P. Champeil, PNAS, **96**, 13750 (1999). 615